ISSN 1070-3284, Russian Journal of Coordination Chemistry, 2018, Vol. 44, No. 1, pp. 82–89. © Pleiades Publishing, Ltd., 2018.

Synthesis, Crystal Stuctures, and Properties of Two 1D Cadmium(II) Coordination Polymers Based on Ferrocenylcarboxylate[1]

S. M. Wang[a, b, c], X. L. Sun[d], X. Y. Zheng[b], Y. X. Feng[e], J. P. Li[b, *], and Z. Y. Liu[b, *]

[a] *Department of Material and Chemistry Engineering, Henan Institute of Engineering, Henan, 451191 P.R. China*

[b] *The College of Chemistry and Molecular Engineering, Zhengzhou University, Henan, 450052 P.R. China*

[c] *Zhengzhou Sino-Crystal Diamond Compand Limited, Henan, 450052 P.R. China*

[d] *Medical Instrument Testing Institute of Hennan Province, Henan, 450003 P.R. China*

[e] *Zhengzhou Foreign Language School, Henan, 450001 P.R. China*

**e-mail: ljp-zd@163.com*

Received March 26, 2017

Abstract—Self-assemblies of the flexible ferrocenyl block 2-chloro-4-ferrocenylbenzoate with Cd^{2+} cations in the presence of N-containing auxiliary ligand result in two coordination complexes, namely, $\{[Cd(\eta^2\text{-}OOCClH_3C_6Fc)_2(Mbbz)(CH_3OH)] \cdot (H_2O)_{0.5}\}_n$ (**I**) and $[Cd(\eta^2\text{-}OOCClH_3C_6Fc)_2(Bbbm)]_n$ (**II**) {Fc = $(\eta^5\text{-}C_5H_4)Fe(\eta^5\text{-}C_5H_4)$, Mbbz = 1,1'-methyl benzimidazole, Bbbm = 1,4-bis(benzimidazol-1-ylmethyl)-benzene}. Their structure has been determined by single-crystal X-ray diffraction analyses (CIF files nos. 1529095 (**I**), 1529096 (**II**)) and further characterized by elemental analyses, IR spectra, and thermogravimetric analyses. Crystallographic characterization shows that both **I** and **II** are 1D chain structures. Notably, various C–H···π interactions and C–H···Cl interactions are discovered in **I** and **II**, and they have significant contributions to self-assembly, which extend 1D complex to infinite 3D supramolecular networks. Moreover, the electrochemical studies of **I** and **II** in DMF solution display irreversible redox waves and indicate that the half-wave potentials of the ferrocenyl moieties in **I** and **II** are shifted to positive potential compared with that of free 2-chloro-4-ferrocenylbenzoate.

Keywords: crystal structure, C–H···π interaction, electrochemistry, ferrocenyl carboxylate

DOI: 10.1134/S1070328417120119

INTRODUCTION

Coordination polymers (CPs), which consist of metal nodes connected by organic ligands, have become one of the research hotspots in the field of coordination chemistry, crystal engineering, supermolecular chemistry and materials chemistry recently [1–5]. The main reasons for peoples' interest in CPs stem from the intriguing variety of structural diversity and from the potential applications to heterogeneous catalysis, molecular recognition, magnetism, gas storage, nonlinear optics and electrical conductivity. Although had made a great progress on the preparation of particular CPs with charming preperties from theoretical and experiment aspects, it is still a challenge to obtain the desired CPs since various factors influence the final target crystalline products, such as the organic ligand, metal ion, ratio of reactant, and so on [6–10]. Among them, rational selection of organic ligands and central metal ions are significant. Organic ligands with donor atoms, such as oxygen and nitrogen, often used to build particular architectures and tune the properties of CPs for the strong coordination ability and stable structures. As a kind of O-donor ligand, carboxylates derivatives is a class of multidentate ligand and has been employed extensively in construction of extended structure. Through the linkage with aromatic ferrocene, carboxylate derivatives can be used as multifunctional ligand for different coordination and hydrogen-bonding interactions and impart interesting features such as good electrochemical properties [11–13]. Furthermore, as a kind of useful second linker, nitrogen contained ligand such as benzimidazole moiety connected by flexible alkyl chain can adopt varied coordination modes and always used to construction fascinating structural frameworks [12–14].

Inspired by forgoing ideas, herein, by using 2-chloro-4-ferrocenylbenzoate as the major ligand and two nitrogen-heterocyclic ligands (Scheme 1) as the second metal linkers, we have successfully obtained two Cd(II) complexes (Scheme 2). The syntheses, crystal structures and thermal properties of the two complexes $\{[Cd(\eta^2\text{-}OOCClH_3C_6Fc)_2(Mbbz)(CH_3OH)] \cdot (H_2O)_{0.5}\}_n$ (**I**) and $[Cd(\eta^2\text{-}$

[1] The article is published in the original.

$OOCClH_3C_6Fc)_2(Bbbm)]_n$ **(II)** {Fc = $(\eta^5\text{-}C_5H_4)Fe(\eta^5\text{-}C_5H_4)$, Mbbz = 1,1'-methyl benzimidazole, Bbbm = 1,4-bis(benzimidazol-1-ylmethyl)-benzene} are discribed in this report. Moreover, the electrochemical behaviors of **I** and **II** are also investgated.

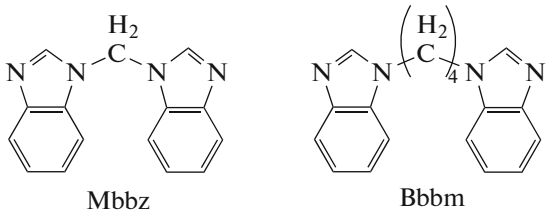

Scheme 1.

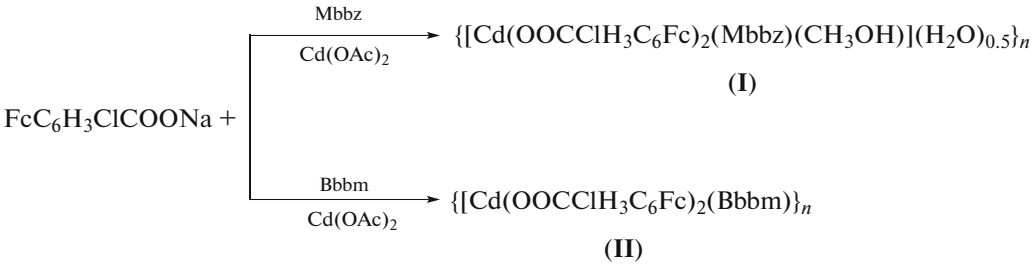

Scheme 2.

EXPERIMENTAL

Materials and methods. We prepared 2-chloro-4-ferrocenylbenzoate and corresponding sodium salt according to literature methods [15], 1,1'-methyl benzimidazole(Mbbz) and Bbbm according to the literatures [16]. All other chemicals were obtained from commercial sources and used without further purification. The analysis of carbon, hydrogen and nitrogen was conducted on a FLASH EA 1112 elemental analyzer. IR spectra were taken on a BRUKER TENSOR 27 spectrophotometer with KBr pellets in 400–4000 cm^{-1} region. TG-DSC measurements were performed by heating samples of **I** and **II** from 30–820°C at a rate of 10°C/min in air on a NETZSCH STA 409PC differential thermal analyzer. Cyclic voltammetric experiments were performed by employing a CHI 660B electrochemical analyzer. There was a three-electrode system composed of a platinum working electrode, a platinum wire auxiliary electrode, and an Ag/AgCl reference electrode. The measurements were conducted in DMF solutions with the tetrabutyl ammonium perchlorate ($n\text{-}Bu_4NClO_4$) (0.1 mol dm^{-3}) as supporting electrolyte. The working electrode was polished to prevent fouling. Pure N_2 gas bubbled through the electrolytic solution was to remove oxygen.

Synthesis of $\{[Cd(\eta^2\text{-}OOCClH_3C_6Fc)_2(Mbbz)(CH_3OH)] \cdot (H_2O)_{0.5}\}_n$ (I). The methanol solution (4 mL) of adjuvant ligand 1,4-bis(benzimidazol-1-ylmethyl)-benzene} (Mbbz) (12.4 mg, 0.05 mmol) was added to a methanol solution (4 mL) of $Cd(OAc)_2 \cdot 2H_2O$ (13.4 mg, 0.05 mmol), and then the methanol solution (3 mL) of $FcC_6H_4ClCOONa$ (36.7 mg, 0.10 mmol) was added to above mixture. The mixture was stirred and then filtered. Then the mixture solution was kept in the dark at room temperature for one week, good quality red crystals were obtained from the resultant red solution. The yield was 48%.

For $C_{25}H_{13}N_5O_4Zn$

anal. calcd., %	C, 55.67	H, 3.61	N, 5.19
Found, %	C, 55.69	H, 3.62	N, 5.11

IR spectrum (KBr; ν, cm^{-1}): 3431 w, 3106 w, 1601 s, 1503 s, 1400 s, 1290 w, 1247 m, 1196 m, 1105 w, 1044 w, 998 w, 791 m, 739 s, 670 w, 594 w, 487 s, 423 w.

Synthesis of $[Cd(\eta^2\text{-}OOCClH_3C_6Fc)_2(Bbbm)]_n$ (II). The methanol solution (4 mL) of adjuvant ligand Bbbm (14.6 mg, 0.05 mmol) was added to a methanol solution (4 mL) of $Cd(OAc)_2 \cdot 2H_2O$ (13.4 mg, 0.05 mmol), and then the methanol solution (3 mL) of $FcC_6H_4ClCOONa$ (36.7 mg, 0.10 mmol) was added to above mixture. The mixture was stirred and then filtered. Then the mixture solution was kept in the dark at room temperature for one week, good quality red

Table 1. Crystallographic data and structure refinement for complexes **I** and **II**

Parameter	Value	
	I	**II**
Fw	1078.85	2160.77
Temperature, K	296(2)	296(2)
Crystal system	Triclinic	Triclinic
Space group	$P\bar{1}$	$P\bar{1}$
a, Å	10.884(2)	13.480(3)
b, Å	11.525(2)	19.116(4)
c, Å	21.351(4)	19.418(4)
α, deg	78.16(3)	81.82(3)
β, deg	84.57(3)	73.75(3)
γ, deg	70.92(3)	73.68(3)
V, Å^3	2476.1(9)	4598.9(16)
Z	1	4
ρ_{calcd}, g cm^{-3}	1.447	1.560
F(000)	1090	2186
θ Range for data collection, deg collection(deg)	2.23–25.00	3.04–25.00
Reflections collected/unique	20146/8641	46538/16094
Data/restraints/params	8641/0/587	16094/120/1231
Goodness-of-fit on F^2	1.060	1.091
Final R_1, wR_2*	0.0721, 0.1558	0.0749, 0.1437

* $R_1 = ||F_o|-|F_c||/|F_o|$. $wR_2 = [w(|F_o^2| - |F_c^2|)^2/w|F_o^2|^2]^{1/2}$. $w = 1/[\sigma^2(F_o)^2 + 0.0297P^2 + 27.5680P]$, where $P = (F_o^2 + 2F_c^2)/3$.

crystals were obtained from the resultant red solution. The yield was 48%.

For $C_{104}H_{81}N_8O_8Cl_4Fe_4Cd_2$			
anal. calcd., %	C, 57.76	H, 3.75	N, 5.18
Found, %	C, 57.48	H, 3.77	N, 5.04

IR spectrum (KBr; ν, cm^{-1}): 3425 m, 1602 s, 1403 m, 1081 w, 1042 w, 832 w, 774 w, 485 m.

X-ray structure determination. The diffraction intensity data of **I** and **II** was collected by a Rigaku RAXIS-IV and SATURN-724 imaging plate area detector with graphite monochromated MoK_α radiation (λ = 0.71073 Å) at room temperature. The structure was solved by direct methods and expanded with Fourier techniques. The non-hydrogen atoms were refined anisotropically. Hydrogen atoms were included but not refined. The final cycle of full-matrix least-squares refinement was based on observed reflections and variable parameters. All calculations were performed by using SHELX-97 crystallographic software package [17]. Table 1 showed crystallographic crystal data and processing parameters for complex **I** and **II** and Table 2 listed corresponding selected bond lengths and bond angles.

Supplementary material for structures has been deposited with the Cambridge Crystallographic Data Centre (CCDC nos. 1529095 (**I**), 1529096 (**II**); www.ccdc.cam.ac.uk/data-request/cif).

RESULTS AND DISCUSSION

The X-ray crystallographic analysis reveals that complex **I** is a 1D chain structure. According to Fig. 1a, Cd(II) metal center is surrounded by two nitrogen atoms (N(1), N(3)) from two benzimidazole rings of symmetry-related mbbz ligands, four oxygen atoms from two $FcClC_2H_4COO^-$, one oxygen atom from a coordinated methanol molecular, forming a $[N_2O_5]$ pentagonal-bipyramidal geometry. Two nitrogen atoms (N(1), N(3)) occupy the axial positions with N(1)Cd(1)N(3) angles of 176.3°, while four atoms O(1), O(2), O(3), O(4), and O(5) comprise the equatorial plane. $FcClC_2H_4COO^-$ anions in **I** coordinate to Cd(II) metal center with the carboxylic group in a chelating mode. The two symmetry-related mbbz groups, exhibiting two benzimidazole rings at two side of the CH_2 core with dihedral angles of 74.23° between

Table 2. Selected bond lengths (Å) and bond angles (deg) of **I** and **II***

Bond	*d*, Å	Bond	*d*, Å
		I	
Cd(1)–O(5)	2.299(5)	Cd(1)–O(1)	2.366(6)
Cd(1)–N(1)	2.300(5)	Cd(1)–O(2)	2.576(6)
Cd(1)–N(3)	2.327(5)	Cd(1)–O(4)	2.572(5)
Cd(1)–O(3)	2.355(5)		
		II	
Cd(1)–N(1)	2.256(5)	Cd(2)–N(8)$^{\#2}$	2.255(5)
Cd(1)–N(4)$^{\#1}$	2.268(5)	Cd(2)–N(5)	2.269(5)
Cd(1)–O(3)	2.317(5)	Cd(2)–O(6)	2.342(5)
Cd(1)–O(1)	2.372(15)	Cd(2)–O(5)	2.427(5)
Cd(1)–O(4)	2.421(5)	Cd(2)–O(8)	2.525(13)
Cd(2)–O(7)	2.24(2)		
Angle	ω, deg	Angle	ω, deg
		I	
O(5)Cd(1)N(1)	91.3(2)	O(5)Cd(1)O(4)	85.01(18)
O(5)Cd(1)N(3)	90.5(2)	N(1)Cd(1)O(4)	86.68(19)
N(1)Cd(1)N(3)	176.2(2)	N(3)Cd(1)O(4)	90.1(2)
O(5)Cd(1)O(3)	137.91(19)	O(1)Cd(1)O(4)	141.82(19)
N(1)Cd(1)O(3)	86.88(19)	O(5)Cd(1)O(2)	81.2(2)
N(3)Cd(1)O(3)	89.5(2)	N(1)Cd(1)O(2)	90.3(2)
O(5)Cd(1)O(1)	133.11(19)	N(3)Cd(1)O(2)	93.3(2)
N(1)Cd(1)O(1)	93.2(2)	O(3)Cd(1)O(2)	140.84(19)
N(3)Cd(1)O(1)	88.0(2)	O(1)Cd(1)O(2)	52.19(19)
O(3)Cd(1)O(1)	88.95(19)	O(4)Cd(1)O(2)	165.79(18)
O(3)Cd(1)O(4)	52.90(17)		
		II	
Cd(1)N(1)	2.256(5)	Cd(2)N(8)$^{\#2}$	2.255(5)
Cd(1)N(4)$^{\#1}$	2.268(5)	Cd(2)N(5)	2.269(5)
Cd(1)O(3)	2.317(5)	Cd(2)O(6)	2.342(5)
Cd(1)O(1)	2.372(15)	Cd(2)O(5)	2.427(5)
Cd(1)O(4)	2.421(5)	Cd(2)O(8)	2.525(13)
Cd(2)O(7)	2.24(2)		

* Symmetry transformations used to generate equivalent atoms: $^{\#1}$ $x + 1, y, z$; $^{\#2}$ $x - 1, y, z$ (**II**).

benzimidazole ring (C(35), N(2), C(36), C(37), N(1)) and benzimidazole ring (C(42), N(3), C(43), C(44), N(4)). The symmetry-related Mbbz ligands act as bridges between adjacent metal centers leading to M···M distances of 10.884(2) Å. The range of Cd–O bond lengthsfall in 2.299(5)–2.576(6) Å. The Cd(1)–N(1) and Cd(1)–N(3) bond lengths are 2.300(5) and 2.327(5) Å, respectively [18, 19]. 1D chain which is formed by mbbz ligands bridging Cd(II) metal centers along the *x* direction, are further coordinated with $FcClC_2H_4COO^-$ anions by two kinds of $FcClC_2H_4COO^-$ anions act as paddles associated up and down the 1D chain. Pairs of 1D chains are oppositely arranged into 1D ranbon structure (Fig. 1b) via the intermolecular edge-to-face C–H···π interactions. The ferrocene ring (Cg1 = {C(8)–C(12)}) and phenyl ring (Cg2 = {C(2)–C(7)}) act as centroids for the C–H···π interactions, namely, H(29)···Cg1 and with H(31)···Cg2 distances of 2.97 and 3.19 Å. The intramolecular C–H···Cl interactions are found in **I**, which the hydrogen atoms belong to carbon atoms (C(42), C(35)) of benzimidazole ring, C(42)–H(42)···Cl(1), C(35)–H(35)···Cl(2) hydrogen bonds with H···Cl distances of 2.71 and 2.86 Å, bond angles

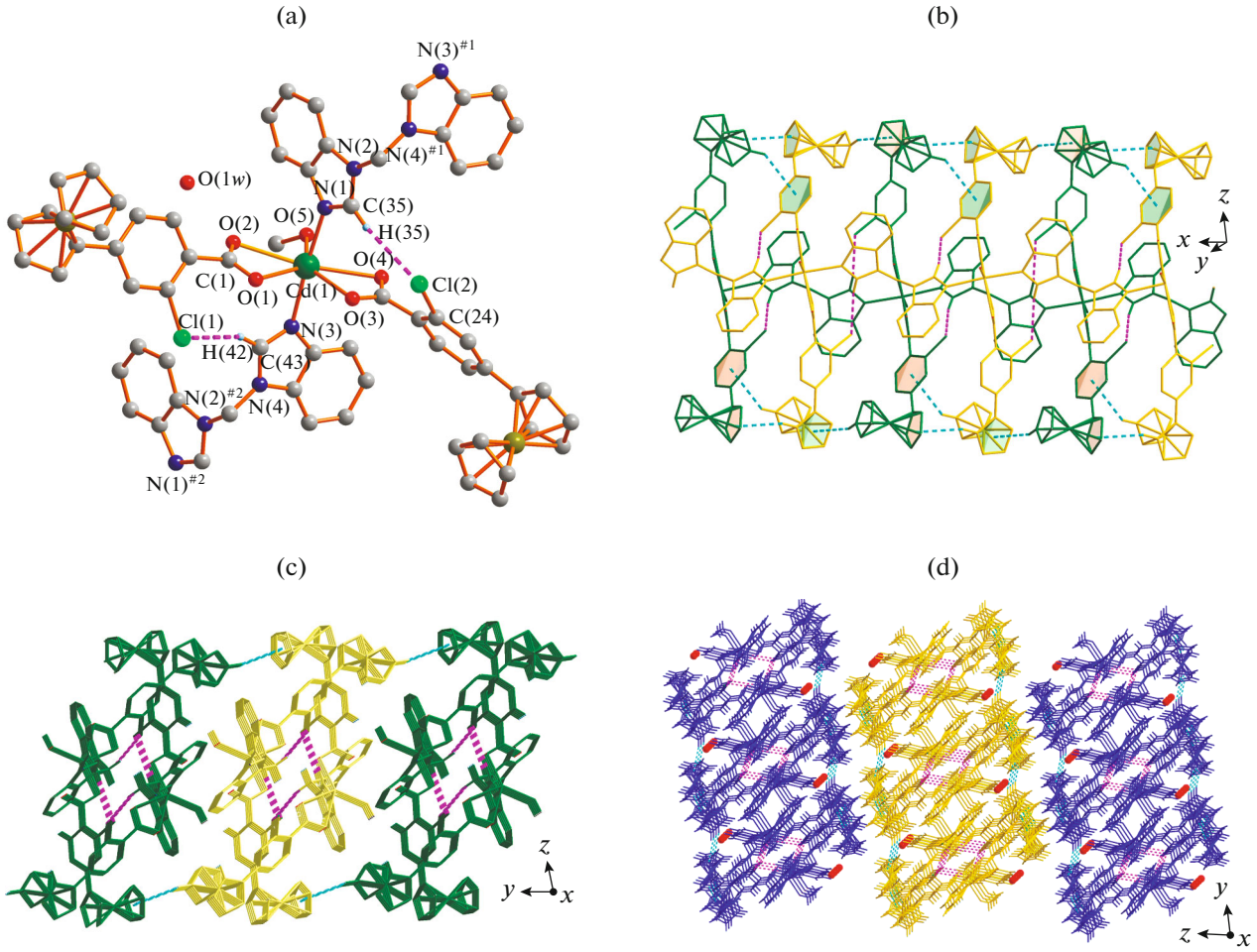

Fig. 1. Coordination environment of **I** (a); the weak C–H···Cl hydrogen bonds and C–H···π stacking interactions in 1D ribbon structure (partial $FcC_6H_3ClCOO^-$ units and hydrogen atoms are omitted for clarity) (b); a view of the 2D supramolecular framework of **I** (c); 3D supramolecular network of complex **I** (the dashed lines represent weak interactions, hydrogens and solvent molecules are omitted for clarity) (d).

of C(42)–H(42)···Cl(1), C(35)–H(35)···Cl(2) are 157° and 170°. These 1D ranbons are paralled to each other into 2D supramolecular structure along the *y* axis (Fig. 1c) via intermolecular interactions of C–H···π (H(15)···Cg3 = 3.04 Å, Cg3 = C(30)–C(34)) interactions. These 2D suparmocular layers are further extended into 3D suparmocular structure by van der Waals interactions (Fig. 1d).

The X-ray crystallographic analysis reveals that complex **II** is a 1D double chain structure. According to Fig. 2a, two Cd(II) metal centers both lie in distorted octahedron coordination geometry. The Cd(II) center is surrounded by four oxygen atoms (O(1), O(2), O(3), O(4) for Cd(1), O(5), O(6), O(7), O(8) for Cd(2) from two different $FcC_6H_3ClCOO^-$ anions and two nitrogen atoms (N(1), $N(4)^{\#1}$ for Cd(1), N(5), $N(8)^{\#2}$ for Cd(2)) from two different Bbbm ligands. The range of Cd–O bond lengths fall in the range of 2.24(2)–2.525(13) Å. The Cd–N bond lengths are in the range of 2.255(5)–2.269(5) Å, respectively [18, 19]. The $FcC_6H_3ClCOO^-$ anions in **II** act as μ_1-bridge in which all the carboxylate groups adopt chelating mode to link Cd(II) metal centers. The Cd(II) metal centers are further bridged by Bbbm ligands to form double paddle-like chains with both of the Cd···Cd distances are 10.884 Å. The intermolecular edge-to-face C–H···π interactions and intramolecular C–H···Cl interactions arranged the double paddle-like chains into 1D ranbon structure (Fig. 2b). The benzimidazole rings (Cg1 = C(88)–C(93), Cg2 = C(36)–C(41)) act as centroids for the C–H···π interactions, namely, $H(42A)^{\#1}$···Cg1 and with $H(94B)^{\#2}$···Cg2 distances of 3.02 and 3.44 Å. The intermolecular C–H···Cl interactions also play a vital role in the 1D ranbon structure forming, which the hydrogen atoms belong to carbon atoms (C(92), C(37)) of benzimidazole ring, C(92)–H(92)···Cl(1), C(37)–H(37)···Cl(4) hydrogen bonds with H···Cl distances of 2.98 and 2.97 Å, bond angles of C(92)–H(92)···Cl(1), C(37)–H(37)···Cl(2) are 154° and 146°.

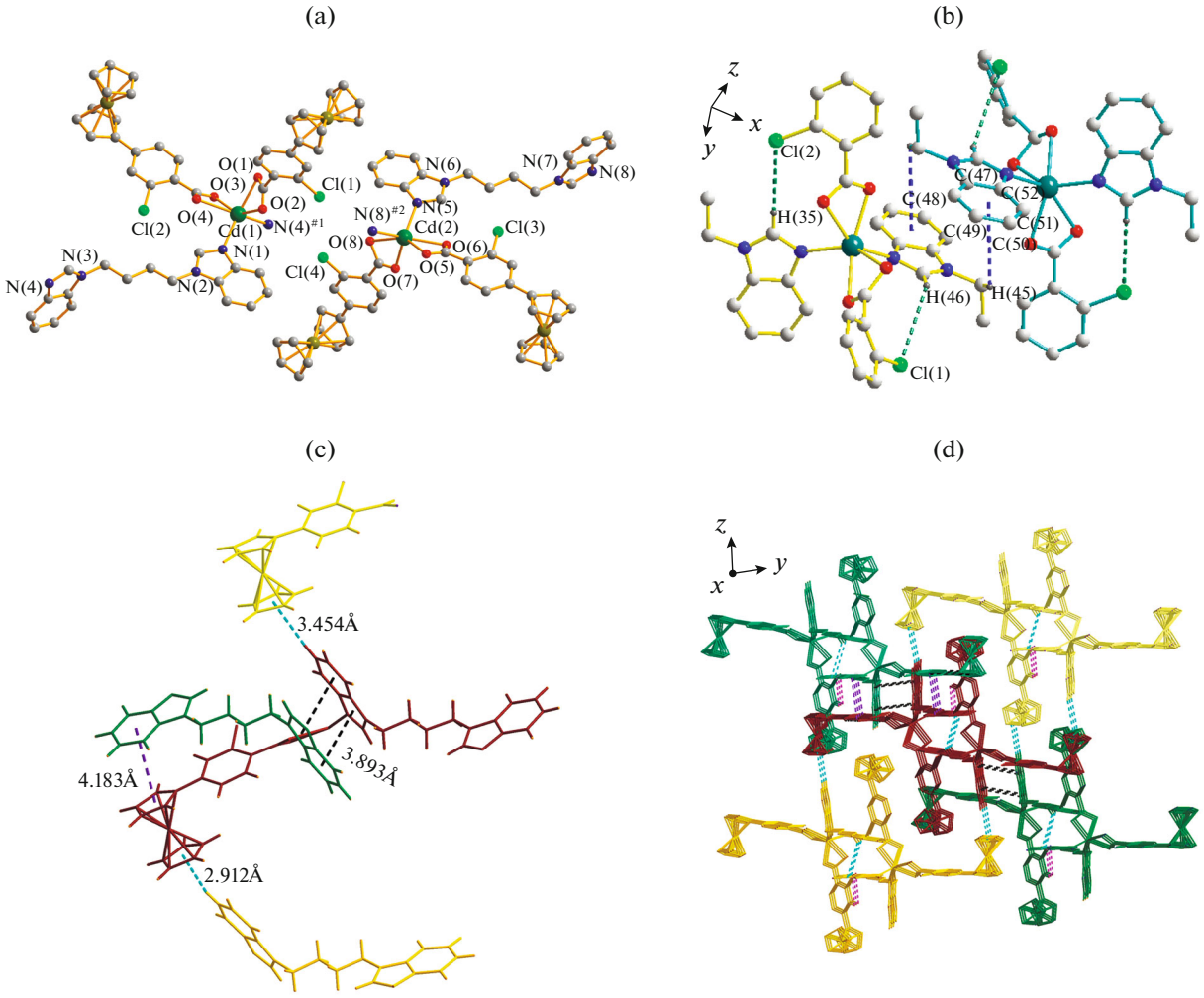

Fig. 2. Coordination environment of **II** (partial Bbbm units and hydrogen atoms are omitted for clarity) (a); notice the weak C–H···Cl hydrogen bonds and C–H···π stacking interactions in 1D ribbon structure (partial Bbbm and $FcC_6H_3ClCOO^-$ units and partial hydrogen atoms are omitted for clarity) (b); notice the weak C–H···π stacking interactions between 1D ribbon structures (partial Bbbm units are omitted for clarity) (c); 3D supramolecular network of complex **II** (the dashed lines represent weak interactions, hydrogens and solvent molecules are omitted for clarity) (d).

Week C–H···Cl interactions: C(43)–H(43*B*)···Cl(2), C(95)–H(95*B*)···Cl(3), hydrogen bonds with H···Cl distances of 3.05 and 3.28 Å, C(43)–H(43*B*)···Cl(2), C(95)–H(95*B*)···Cl(3) bond angles of 120° and 125°, are also found in the individual chains to strength the 1D ranbons (Fig. 2c). These 1D ranbons are further stacked into 3D supramolecular architecture via intermolecular π···π and C–H···π interactions [18]. The π–π stacking interactions exist between the two benzimidazole rings (Cg3 = C(47)–C(52), Cg4 = N(3)–C(47)) of the Bbbm ligand and between the ferrocene ring (Cg5 = C(18)–C(22)) of $FcC_6H_3ClCOO^-$ anion and benzimidazole ring (Cg6 = C(36)–C(41)) of the Bbbm ligand with centroid-centroid distance of Cg3···Cg4 = 3.893 Å and Cg5···Cg6 = 4.029 Å, respectively. In the 3D supramolecular architecture (Fig. 2d), there are two types of intermolecular edge-to-face C–H···π interactions with ferrocene rings act as centroids (Cg7 = C(23)–C(27) ring, Cg8 = C(58)–C(62) ring) for C(101)–H(101)···Cg7 and C(50)–H(50)···Cg8 with distances of 4.029 and 3.454 Å.

The thermal decomposition curves of **I** and **II** are showed in Fig. 3. For **I**, a gradual weight loss between 30 and 185°C is attributed to the release of half a free water molecular and one coordinated methanol molecule (obsd. 3.74%, calcd. 3.71%). Hereafter, the host framework starts to decompose. The decomposition process is completed at 568°C giving brown fine crystalline powder CdO + Fe_2O_3 as the final decomposition product (obsd. 26.66%, calcd. 26.70%). Thermogravimetric (TG) data shows that **II** is stable in the solid state up to approximately 400°C. The TG curves of complex **II** show two continuous weight loss stages from 400–560°C corresponding to the decomposition

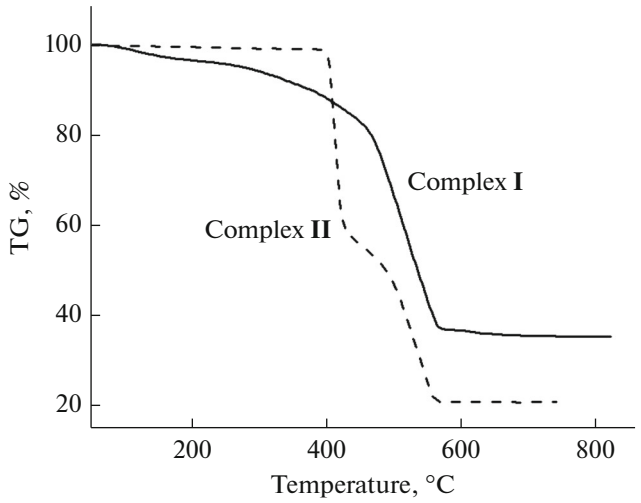

Fig. 3. The thermal decomposition curves of **I** and **II**.

of Bbbm and $FcC_6H_3ClCOO^-$ ligands. Finally, in complex **II**, a plateau region is observed from 560 to 750°C. There remain to be a brown fine crystalline powder of CdO + Fe_2O_3 (obsd. 13.40%, calcd. 13.33%).

The electrochemical behaviors of **I** and **II** has been studied by cyclic voltammetry (CV) and differential pulse voltammograms (DPVs) in DMF (~5.0×10^{-4} mol L^{-1} total Fc concentrations) containing 0.1 mol L^{-1} n-Bu_4NClO_4 as the supporting electrolyte. As shown on Fig. 4a, CVs of **I**, **II** and sodium 2-chloro-4-ferrocenylbenzoate display a couple of quasi reversible redox process, which can be assigned to ferrocenyl moiety. The DPV of sodium 2-chloro-4-ferrocenylbenzoate shift to lower potential (0.544 V) when compared with FcCH=HCOOH (0.620 V in DMF solution) and $FcCOC_2H_4COOH$ (0.716 V in DMF solution) [20]. This change can own to the electron-rich benzene ring makes the 2-chloro-4-ferrocenylbenzoate easier to be oxidized. The solution-state DPVs (Fig. 4b) of **I** and **II** show a single peak with a half-wave potential ($E_{1/2}$ vs. SCE) at 0.554 and 0.556 V. Compared with free $FcC_6H_3ClCOOH$, the potential data of **I** and **II** shifted to higher place. The electron-withdrawing nature of the coordinated metal centers responds to the change, and thus decrease the electron cloud density of the ferrocene unit and makes it hard to be oxidized [21–23]. It also can be noted that **I** and **II** have same half-wave potentials, which can be assigned to the same chemical environment.

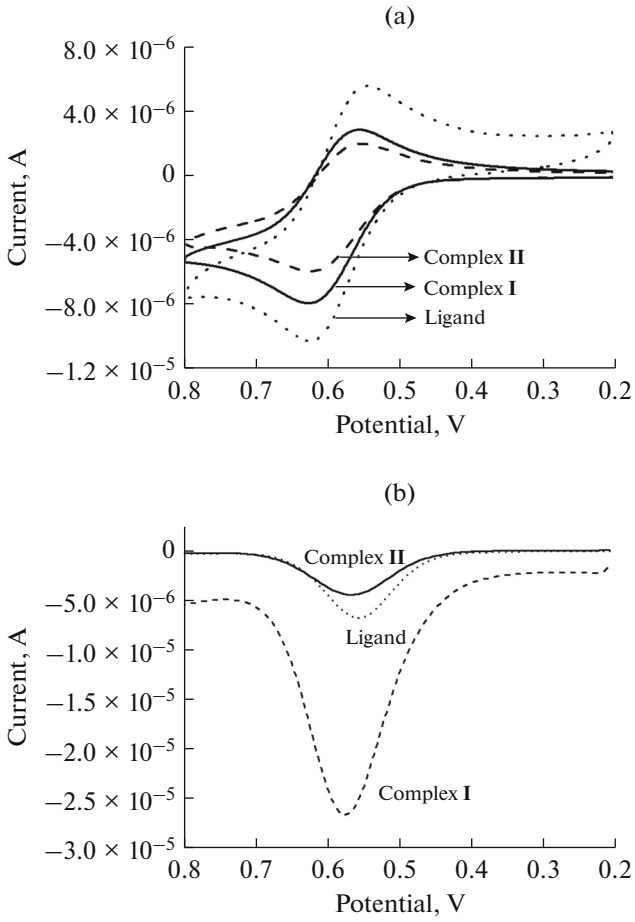

Fig. 4. Cyclic voltammograms (a) and differential pulse voltammograms (b) of complexes **I** and **II**.

ACKNOWLEDGMENTS

We are thankful for financial support from national natural science foundation (nos. 61405054, 21273205, 21543011 and J1210060), Henan province science and technology research program (nos. 162102210167, 172102210483), Key scientific research projects of Henan Province (17A150020).

REFERENCES

1. Hu, S., Meng, Z.S., and Tong, M.L., *Cryst. Growth Des.*, 2010, vol. 10, p. 1742.
2. Lan, Y.Q., Li, S.L., Shao, K.Z., et al., *Cryst. Growth Des.*, 2008, vol. 8, p. 3490.
3. Zhang, Z., Xiang, S., Zheng, Q., et al., *Cryst. Growth Des.*, 2010, vol. 10, p. 2372.
4. Perry, J.J., Perman, J.A., and Zaworotko, M.J., *Chem. Soc. Rev.*, 2009, vol. 38, p. 1400.
5. Li, J.P., Li, L.K., Hou, H.W., et al., *Cryst. Growth Des.*, 2009, vol. 9, p. 4504.
6. Lin, J.B., Zhang, J.P., and Chen, X.M., *J. Am. Chem. Soc.*, 2010, vol. 132, p. 6654.
7. Li, J.R., Kuppler, R.J., and Zhou, H.C., *Chem. Soc. Rev.*, 2009, vol. 38, p. 1477.
8. Shimomura, S., Higuchi, M., Matsuda, R., et al., *Nat. Chem.*, 2010, vol. 2, p. 633.
9. Nouar, F., Eckert, J., Eubank, J.F., et al., *J. Am. Chem. Soc.*, 2009, vol. 131, p. 2864.

10. Zhang, J., Wu, T., Chen, S., et al., *Angew. Chem. Int. Ed.*, 2009, vol. 48, p. 3486.
11. Guo, Z., Li, G., Zhou, L., et al., *Inorg. Chem.*, 2009, vol. 48, p. 8069.
12. Hardi, M.D., Serre, C., Frot, T., et al., *J. Am. Chem. Soc.*, 2009, vol. 131, p. 10857.
13. Li, J.P., Li, X.F., Lu, H.J., et al., *Inorg. Chim. Acta*, 2012, vol. 384, p. 163.
14. Aakeröy, C.B., Desper, J., Leonard, B., et al., *Cryst. Growth Des.*, 2005, vol. 5, p. 865.
15. Broadhead, G.D., Osgerby, J.M., and Pauson, P.L., *J. Chem. Soc.*, 1958, p. 650.
16. Aakeröy, C.B., Desper, J., Leonard, B., et al., *Cryst. Growth Des.*, 2005, vol. 5, p. 865.
17. Sheldrick, G.M., *SHELXTL-97, Program for the Solution and Refinement of Crystal Structures*, Göttingen: Univ. of Göttingen, 1997.
18. Li, J.P., Li, L.K., Hou, H.W., et al., *J. Organomet. Chem.*, 2009, vol. 694, p. 1359.
19. Shi, X.J., Li, Q.X., Zhang, Y.S., et al., *J. Coord. Chem.*, 2011, vol. 64, p. 3918.
20. Li, J.P., Sun, H., Yuan, Q.Q., et al., *J. Coord. Chem.*, 2013, vol. 66, p. 1686.
21. Hou, H.W., Li, L.K., Zhu, Y., et al., *Inorg. Chem.*, 2004, vol. 43, p. 4767.
22. Barranco, E.M., Crespo, O., Gimeno, M.C., et al., *Dalton Trans.*, 2001, p. 2523.
23. Xu, Y.M., Saweczko, P., and Kraatz, H.B., *J. Organomet. Chem.*, 2001, vol. 637, p. 335.